CHAPTER IV
RESULTS AND DISCUSSION

4.1 Catalyst Characterization

4.1.1 Crystal Structures

The XRD patterns of pure TiO_2 as reference and the calculation of crystallite sizes of all studied catalysts are shown in Appendix A. Figure 4.1 shows the XRD patterns of TiO_2 (Degussa P25), TiO_2 (sol-gel-1), TiO_2 (sol-gel-2) and 1.0%Pt/TiO_2. Generally, there are three different forms of TiO_2 namely anatase, rutile and brookite. For the XRD patterns of TiO_2, the main peaks at $2\theta = 25.3^o$, 27.5^o and 30.6^o are for anatase, rutile and brookite, respectively. For the TiO_2 (Degussa P25), anatase and rutile phases were observed. The major phase is anatase and rutile exists as the minor phase. For TiO_2 (sol-gel-1), the anatase peaks were observed as the major phase whereas the brookite one exists as the minor phase. TiO_2 (sol-gel-2) has only the anatase phase. The anatase peak of TiO_2 (Degussa P25) has higher intensity than that of TiO_2 catalysts prepared by the sol-gel method. For 1.0% Pt/TiO_2, there was only TiO_2 in the anatase form and no peaks of Pt at $2\theta = 40^o$, 48^o was observed. It is suggested that Pt can be dispersed well on TiO_2. The XRD patterns of Ag/TiO_2 catalysts at different Ag loadings are shown in Figure 4.2. For Ag/TiO_2 catalysts calcined at 400 ^oC and having 0.2-1.5 mol% Ag, it can be observed that the anatase is the major phase.

The crystallite sizes of the catalysts can be determined from the broadening of the anatase main peak by using the Debye-Scherrer equation. The crystallite sizes of all studied catalysts are given in Table 4.1. The crystallite sizes of both sol-gel TiO_2 catalysts are smaller than that of TiO_2 (Degussa P25). When compared with blank TiO_2 (sol-gel-1), the amount of Ag loading does not significantly affect the crystallite size of the catalysts. However, loading Pt into TiO_2 increases the crystallite size of the catalyst.

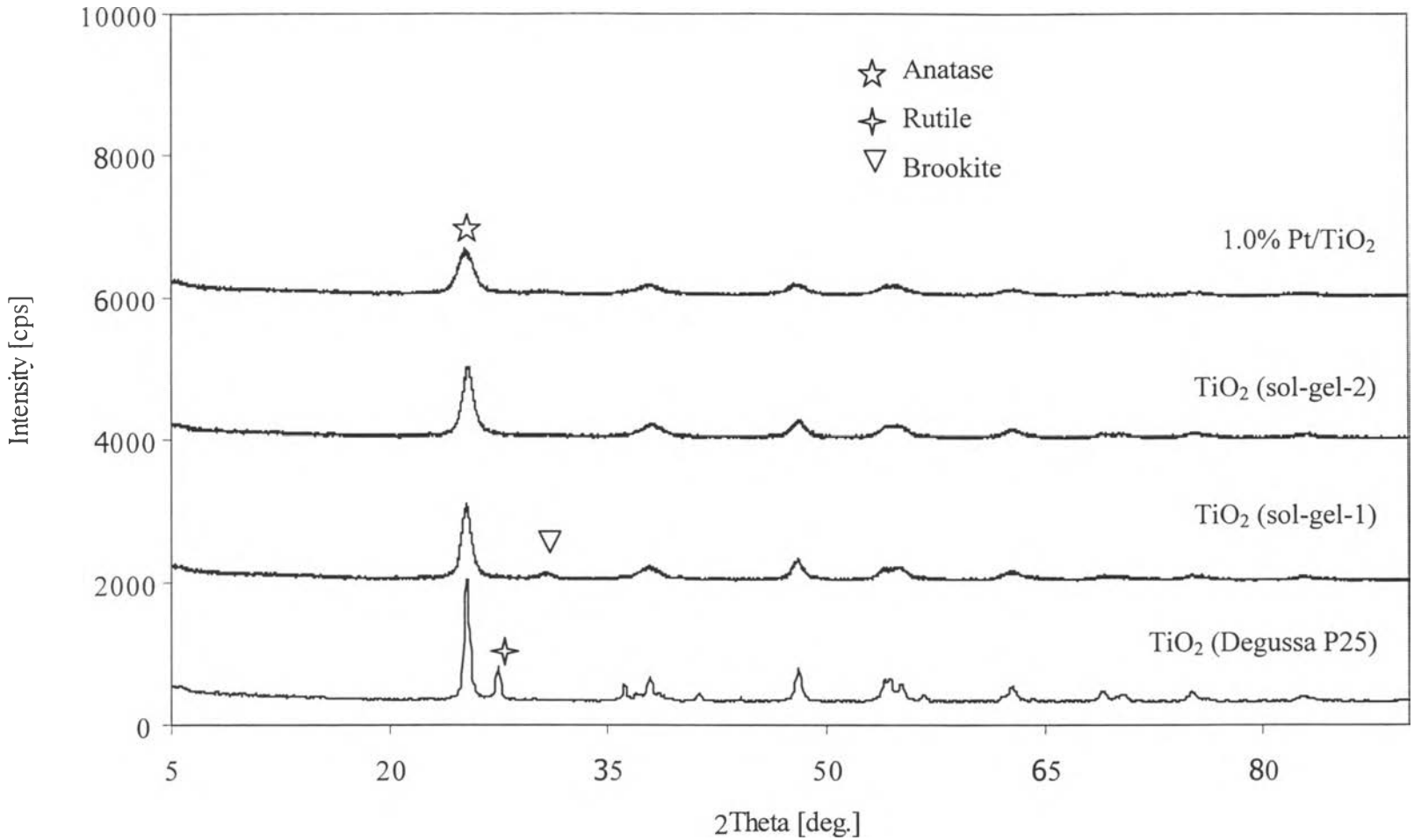

Figure 4.1 X-ray diffraction patterns of TiO_2 (Degussa P25), TiO_2 (sol-gel-1), TiO_2 (sol-gel-2), 1.0% Pt/TiO_2.

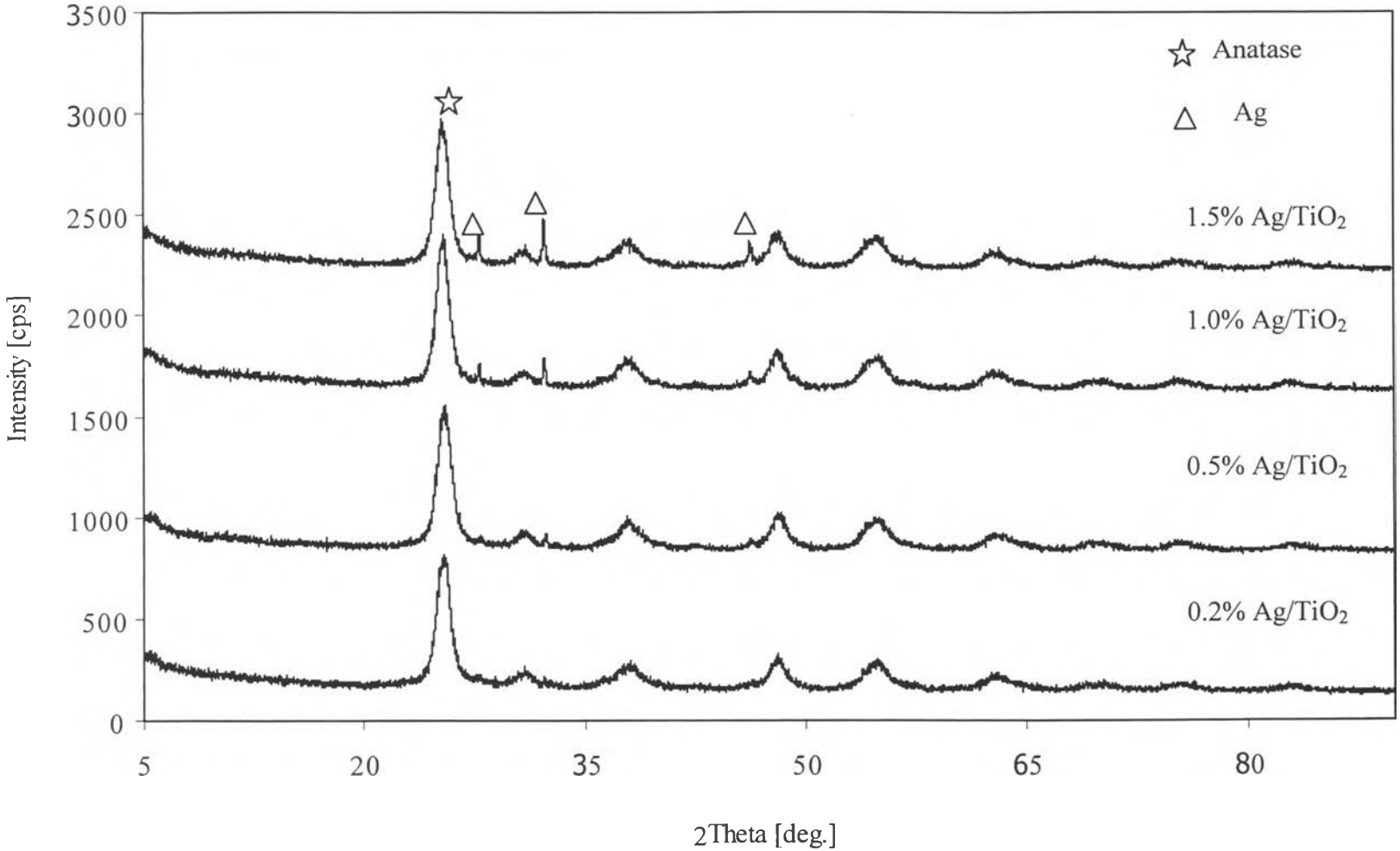

Figure 4.2 X-ray diffraction patterns of Ag/TiO_2 catalyst at different Ag loading.

Table 4.1 Calculated crystallite sizes of the studied catalysts.

Catalyst	Crystallite Size (nm)
TiO_2 (Degussa P25)	24
TiO_2 (sol-gel-1)	13
TiO_2 (sol-gel-2)	11
1.0%Pt/TiO_2 (sol-gel-1)	26
0.2% Ag/TiO_2 (sol-gel-1)	9
0.5% Ag/TiO_2 (sol-gel-1)	11
1.0% Ag/TiO_2 (sol-gel-1)	15
1.5% Ag/TiO_2 (sol-gel-1)	10

4.1.2 Surface Structures

The surface areas, pore volumes and pore sizes of all studied catalysts are shown in Table 4.2. All catalysts prepared by both sol-gel methods have higher BET surface areas and pore volumes than those of TiO_2 (Degussa P25). On the contrary, the pore sizes of pure TiO_2 and 1.0% Pt/TiO_2 prepared by the first sol-gel method are comparable to that of TiO_2 (Degussa P25). An addition of Ag into TiO_2 did not significantly affect the pore size, pore volume, and BET surface area.

Table 4.2 Surface areas, pore sizes and pore volumes of the studied catalysts.

Catalyst	BET Surface Area (m^2/g)	Pore Size (nm)	Pore Volume (cm^3/g)
TiO_2 (Degussa P25)	55.9	6.3	0.092
TiO_2 (sol-gel-1)	101.2	5.9	0.156
TiO_2 (sol-gel-2)	137.1	6.1	0.217
1.0% Pt/TiO_2	112.2	4.5	0.131
0.2% Ag/TiO_2	105.7	8.0	0.219
0.5% Ag/TiO_2	113.5	7.5	0.221
1.0% Ag/TiO_2	105.0	7.3	0.201
1.5% Ag/TiO_2	122.7	7.0	0.220

4.1.3 Surface Morphology

The surface characteristics and the particle sizes of the studied catalysts were studied using SEM and TEM. Figure 4.3 shows the scanning electron micrographs of all catalysts. It is clearly seen from Figure 4.3 that the TiO_2 catalysts prepared by both sol-gel methods have a high degree of agglomeration of primary particles. Figure 4.4 shows the transmission electron micrographs of TiO_2 (sol-gel-1) compared to TiO_2 (Degussa P25). The primary particle sizes of (Degussa P25) and TiO_2 (sol-gel-1) are ca 20 nm and 10 nm, respectively, and consistent with the results reported in Table 4.1. As seen in Figure 4.4 (c), the aggregates consist of primary particles to form secondary particles, which have the particle size around 182 nm.

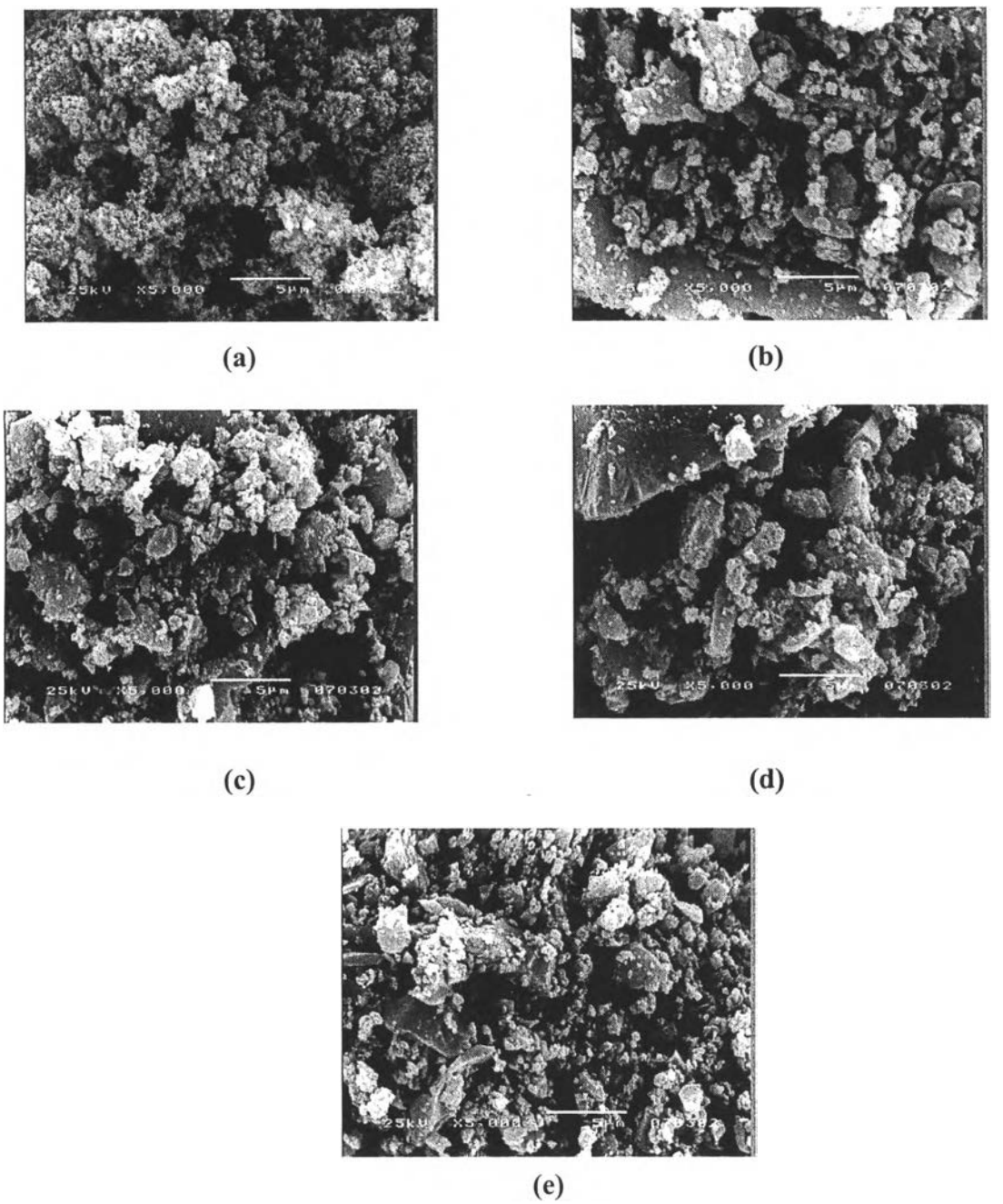

Figure 4.3 Scanning electron micrographs at 5,000 × magnification of (a) TiO_2 (Degussa P25), (b) TiO_2 (sol-gel-1), (c) TiO_2 (sol-gel-2), (d) 1.0% Pt/TiO_2 and (e) 0.5% Ag/TiO_2.

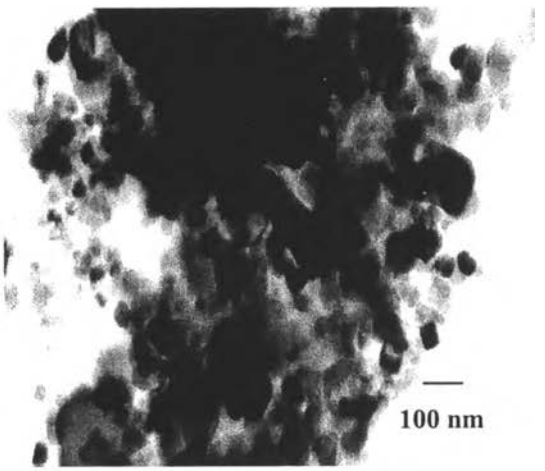

(a)

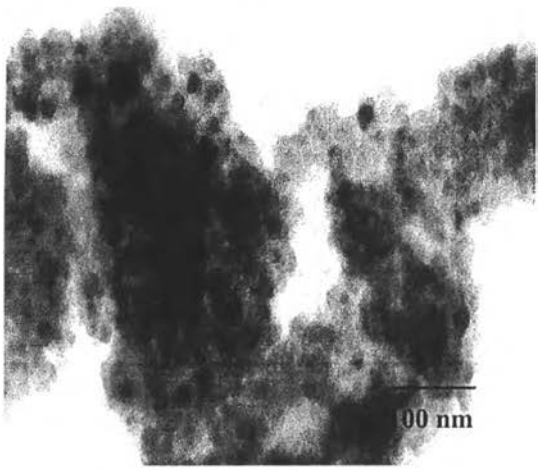

(b)

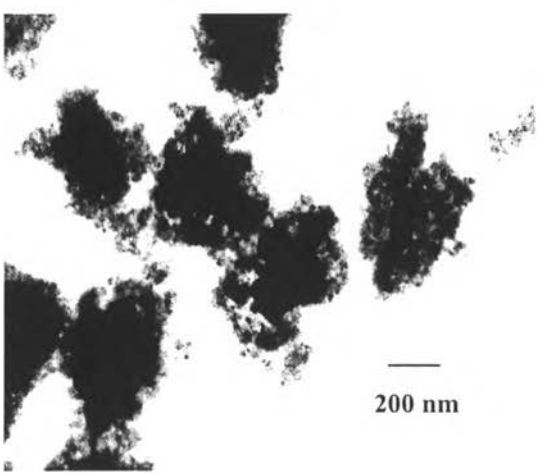

(c)

Figure 4.4 Transmission electron micrographs of (a) TiO_2 (Degussa P25) at 150,000 × magnification, (b) TiO_2 (sol-gel-1) at 300,000 × magnification and (c) TiO_2 (sol-gel-1) at 84,000× magnification.

4.2 Photocatalytic Degradation of 4-chlorophenol

Some nomenclatures used throughout this section are the remaining fraction of 4-CP (C/C_0) and the remaining fraction of TOC (TOC/TOC_0). C/C_0 is the ratio of 4-CP concentration at any time to its initial concentration. TOC/TOC_0 is the ratio of TOC concentration at any time to its initial concentration. The experimental data of the photocatalytic activities of all studied catalysts are shown in Appendix B.

4.2.1 Photocatalytic Degradation of 4-CP with TiO_2

4.2.1.1 Effect of TiO_2 (Degussa P25)

Photocatalytic degradation of 0.5 mM 4-CP solution was carried out with TiO_2 (Degussa P25) loading of 0.5 g/l under UV irradiation. Samples were taken every 30 minutes to analyze for the concentration of 4-CP and other products. Figure 4.5 shows the remaining fractions of 4-CP and TOC without any catalyst but with pure oxygen aeration. It was found that 4-CP decreases sharply and disappears after 90 minutes but the TOC decreases only 38% after the irradiation for 360 minutes. In the presence of TiO_2 (Degussa P25) and with pure oxygen aeration, the TOC decreases 93% from the initial TOC after the irradiation for 360 minutes as shown in Figure 4.6. However, 4-CP could not be completely degraded with TiO_2 (Degussa P25). The remaining 4-CP in solution is approximatly around 0.0056 mM. Remarkably, the intermediate concentrations of hydroquinone (HQ) and hydroxyhydroquinone (HHQ) reaches the maximum values at 90 and 120 minutes, respectively, when TiO_2 (Degussa P25) was added and the solution was aerated with pure oxygen. In addition, the concentrations of intermediate products are much lower than those without catalyst. It can be concluded that the UV lamp with the short wavelength destroys the chemical bond in the 4-CP molecule and transforms into the intermediate products rather than CO_2 and an addition of TiO_2 catalyst can enhance the degradation rate of 4-CP.

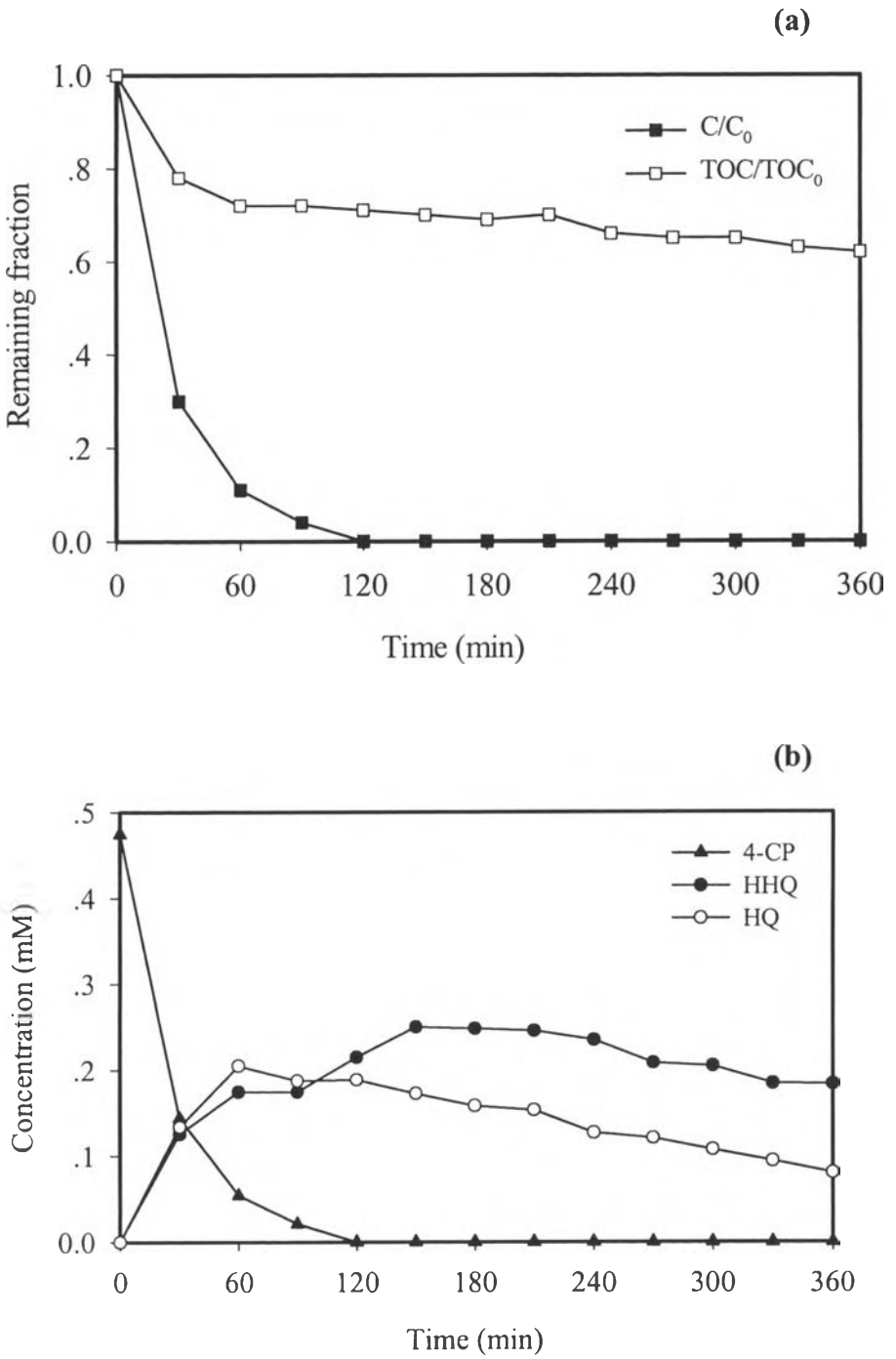

Figure 4.5 Photocatalytic degradation of 4-CP as a function of irradiation time without catalyst under the presence of dissolved oxygen (a) remaining fractions of 4-CP and TOC (b) concentrations of the intermediate products. Experimental conditions: 5 g/l catalyst, 0.5 mM 4-CP, 298 K and 5.5 initial pH.

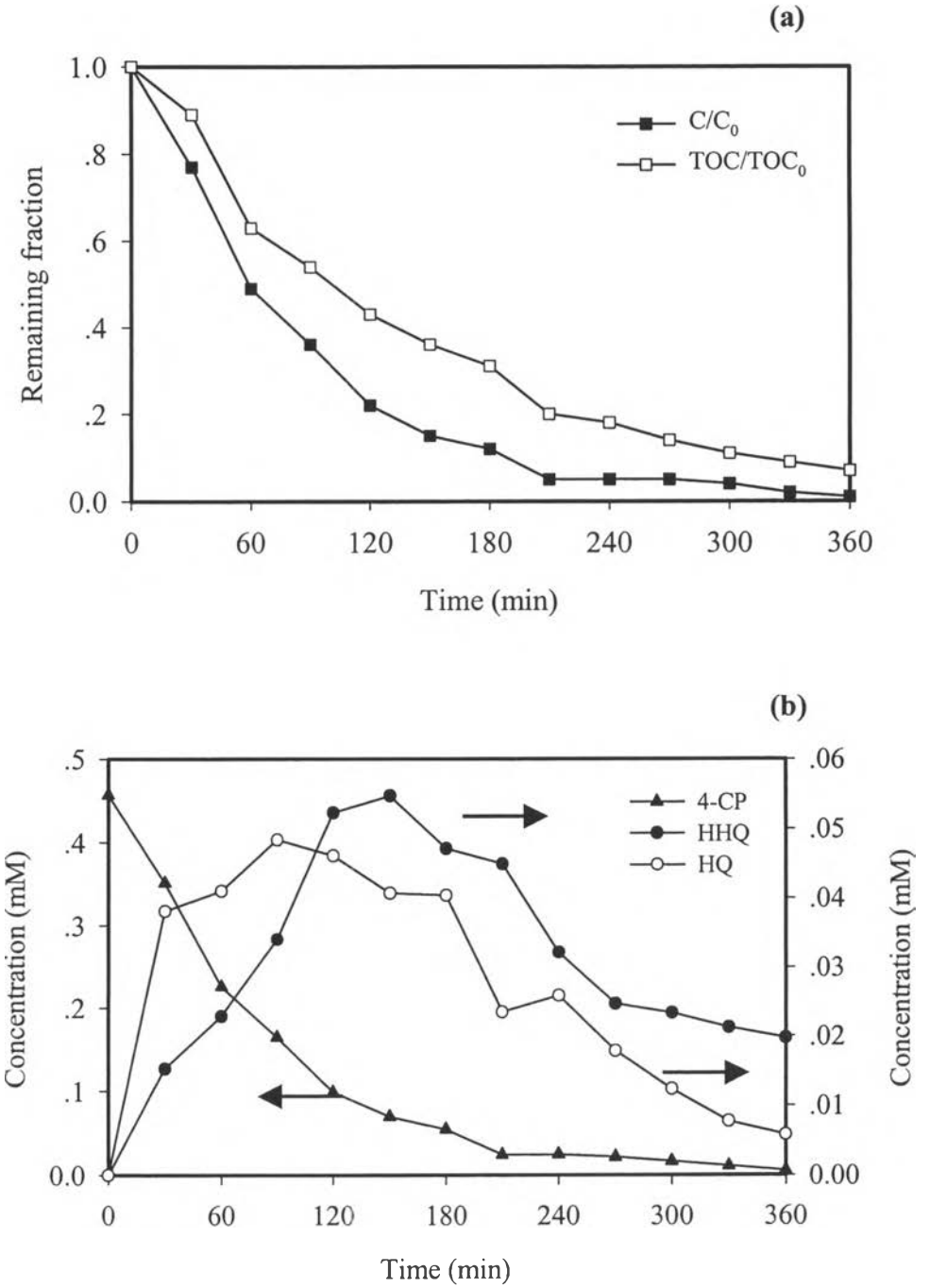

Figure 4.6 Photocatalytic degradation of 4-CP as a function of irradiation time using TiO_2 (Degussa P25) under the presence of dissolved oxygen (a) remaining fractions of 4-CP and TOC (b) concentrations of the intermediate products. Experimental conditions: 5 g/l catalyst, 0.5 mM 4-CP, 298 K and 5.5 initial pH.

4.2.1.2 Effect of TiO_2 (sol-gel)

The photocatalytic degradations of 4-CP with dissolved oxygen condition using TiO_2 prepared by two sol-gel methods are shown in Figures 4.7-4.8. Both TiO_2 catalysts have the same rates of 4-CP degradation and TOC reduction. However, the concentration profiles of the intermediate products were different significantly for the illumination time up to 300 minutes.

Compared with the commercial TiO_2 (Degussa P25), the decrease of 4-CP concentration with either TiO_2 (sol-gel-1) or TiO_2 (sol-gel-2) are much faster and the 4-CP concentration disappears within 90 minutes. However, the TOC degradation rate with TiO_2 (Degussa P25) is higher than those with the sol-gel TiO_2 catalysts. The results imply that the degradation rate of the intermediate products with TiO_2 (Degussa P25) is higher than that with the sol-gel TiO_2 catalysts.

Higher surface areas of both sol-gel TiO_2 catalysts resulted in larger amount of 4-CP adsorbed on the catalyst surface leading to the higher degradation rates of 4-CP as compared to the commercial TiO_2 (Degussa P25). TiO_2 (Degussa P25) gives a higher degradation rate in terms of TOC than TiO_2 (sol-gel) because of its higher crystalinity than both sol-gel TiO_2 catalysts. That, inturn, reduces the e^-/h^+ recombination. When the recombination effect decreases, there are more electrons and holes diffuse to the catalyst surface and react with the substrate molecules adsorbed on the surface at the faster rate (Jung and Park, 2000 and Tharathonpisutthikul, 2000). The results are also consistent with the work done by Guillard *et al.* (1999). They investigated the 4-CP degradation using different TiO_2 catalysts, TiONA PC 10, TiLCOC HC 120, Hombikat UV 100 and Degussa P25. Although the TiO_2 (Degussa P25) had a lowest surface area, it was observed that the TiO_2 (Degussa P25) had the highest TOC degradation rate. It was explained that TiO_2 (Degussa P25) decreased the readsorption rate of the intermediate products.

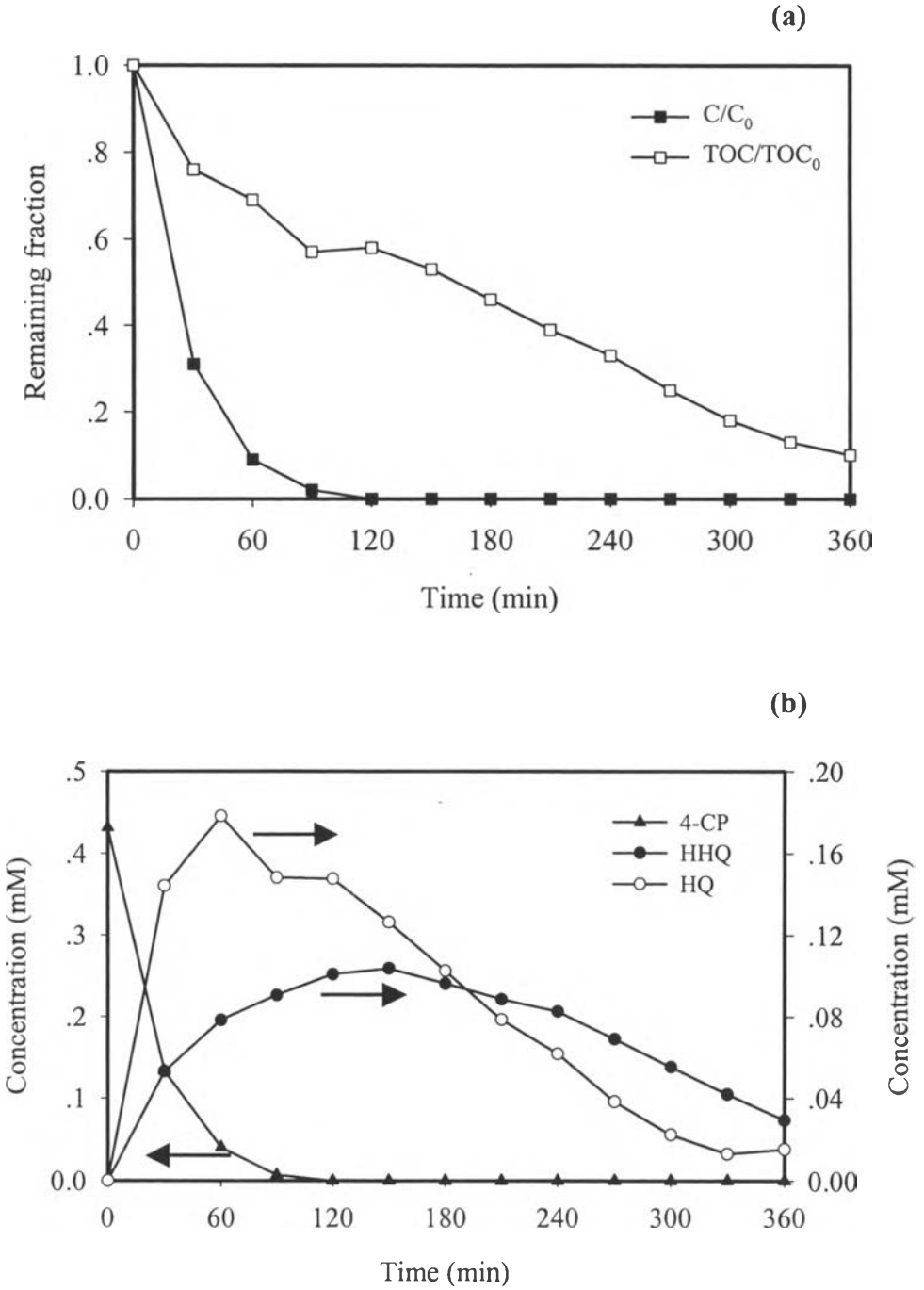

Figure 4.7 Photocatalytic degradation of 4-CP as a function of irradiation time using TiO_2 (sol-gel-1) under the presence of dissolved oxygen (a) remaining fractions of 4-CP and TOC (b) concentrations of the intermediate products. Experimental conditions: 5 g/l catalyst, 0.5 mM 4-CP, 298 K and 5.5 initial pH.

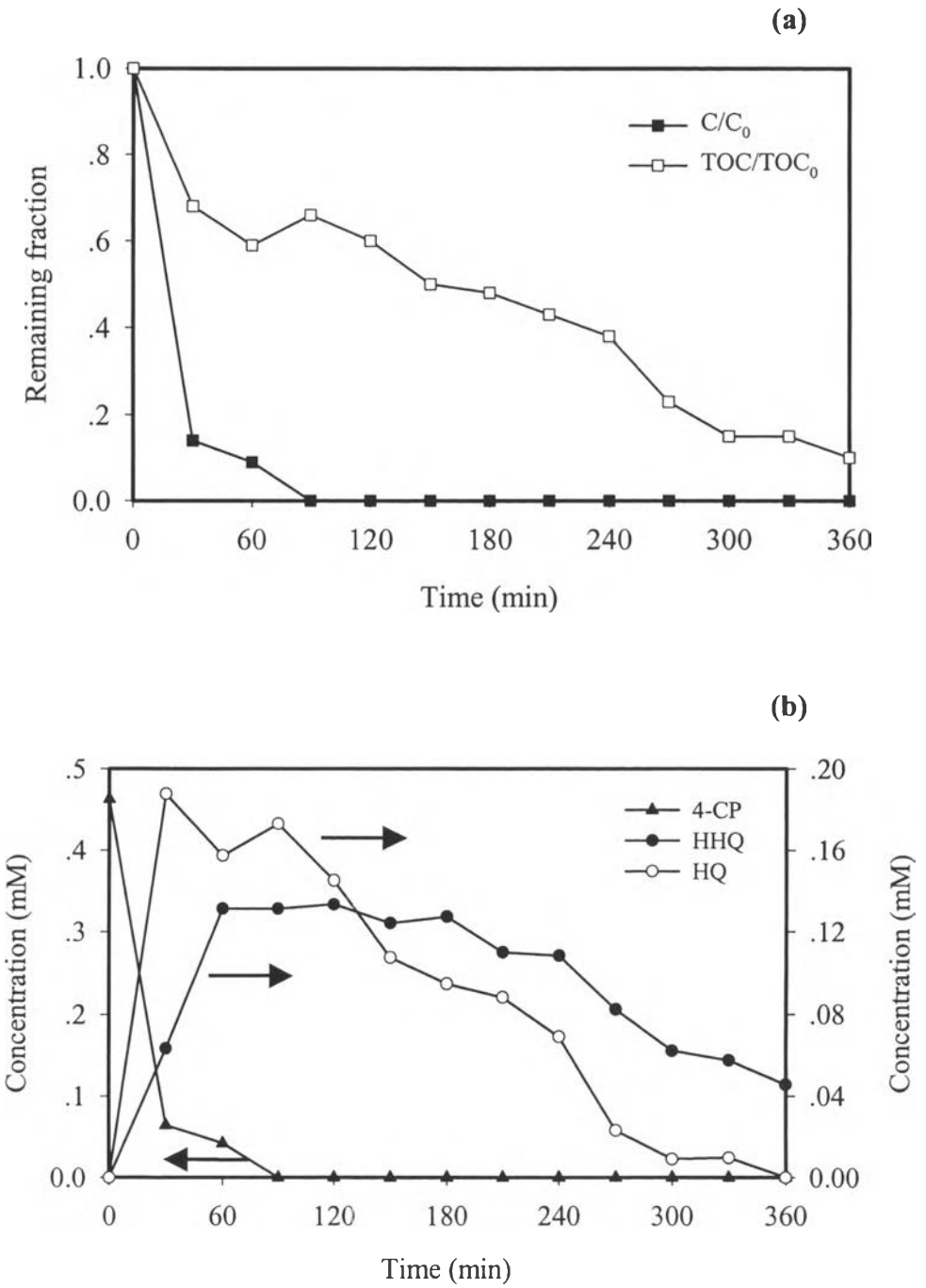

Figure 4.8 Photocatalytic degradation of 4-CP as a function of irradiation time using TiO_2 (sol-gel-2) under the presence of dissolved oxygen (a) remaining fractions of 4-CP and TOC (b) concentrations of the intermediate products. Experimental conditions: 5 g/l catalyst, 0.5 mM 4-CP, 298 K and 5.5 initial pH.

4.2.1.3 Effect of dissolved oxygen

In order to determine the effect of dissolved oxygen on the 4-CP degradation, the solution was aerated with nitrogen to obtain zero dissolved oxygen while other experiments were carried out at a very high dissolved oxygen level by bubbling pure oxygen gas into the solution. Figures 4.9-4.11 illustrate the 4-CP degradation under the absence of dissolved oxygen and without a catalyst, with TiO_2 (Degussa P25) and TiO_2 (sol-gel-1), respectively. The results for the 4-CP degradation under the presence of dissolved oxygen and without a catalyst, with TiO_2 (Degussa P25), TiO_2 (sol-gel-1) are shown in Figures 4.5-4.7, respectively. The remaining fractions of TOC at the irradiation time 360 minutes for each catalyst are shown comparatively in Table 4.3.

As seen from the experimental results, under the presence of dissolved oxygen, the degradation rates of 4-CP and TOC were much higher than those of the systems under the absence of dissolved oxygen for both with and without catalysts. For TiO_2 (sol-gel-1), the three intermediate products, HQ, benzoquinone (BQ) and HHQ were generated during the 4-CP degradation under the absence of dissolved oxygen but BQ was not generated during the 4-CP degradation under the presence of dissolved oxygen. It can be concluded that the dissolved oxygen not only reduces the intermediate concentrations but also reduces the type of the intermediate products.

The presence of dissolved oxygen plays a significant role in the photocatalytic degradation of 4-CP. As explained by Litter (1999), the oxygen molecule can act as an electron scavenger to trap and separate electron out from the positive hole that will help to reduce the chance of electron-hole pair recombination. Furthermore, the oxygen molecule can affect the fate of the photogenerated species. The oxygen molecule reacts with the conduction band electrons to form superoxide anion radical (equation 2.9) reacting further with hydrogen ions to a perhydroxyl radical. Consequently, the perhydroxyl radical can form hydrogen peroxide, which in turn, gives rise to the hydroxyl radical (equations 2.15-2.18) (Reutergardh et al., 1997). Additionally, the oxygen flow serves as the stirring medium performing the mass transfer in the irradiated systems (Blazkova *et al.*, 1998).

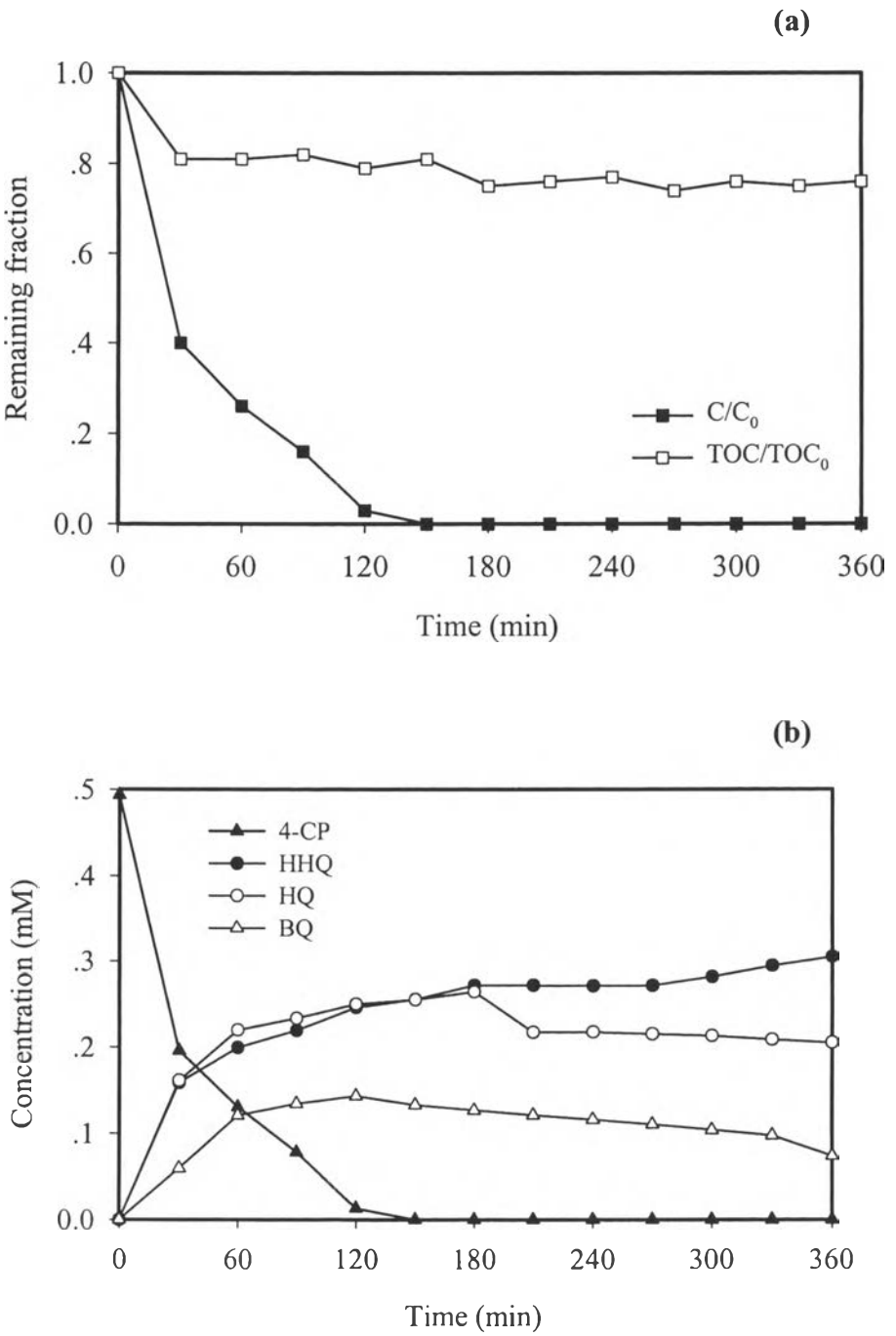

Figure 4.9 Photocatalytic degradation of 4-CP as a function of irradiation time without catalyst under the absence of dissolved oxygen (a) remaining fractions of 4-CP and TOC (b) concentrations of the intermediate products. Experimental conditions: 5 g/l catalyst, 0.5 mM 4-CP, 298 K and 5.5 initial pH.

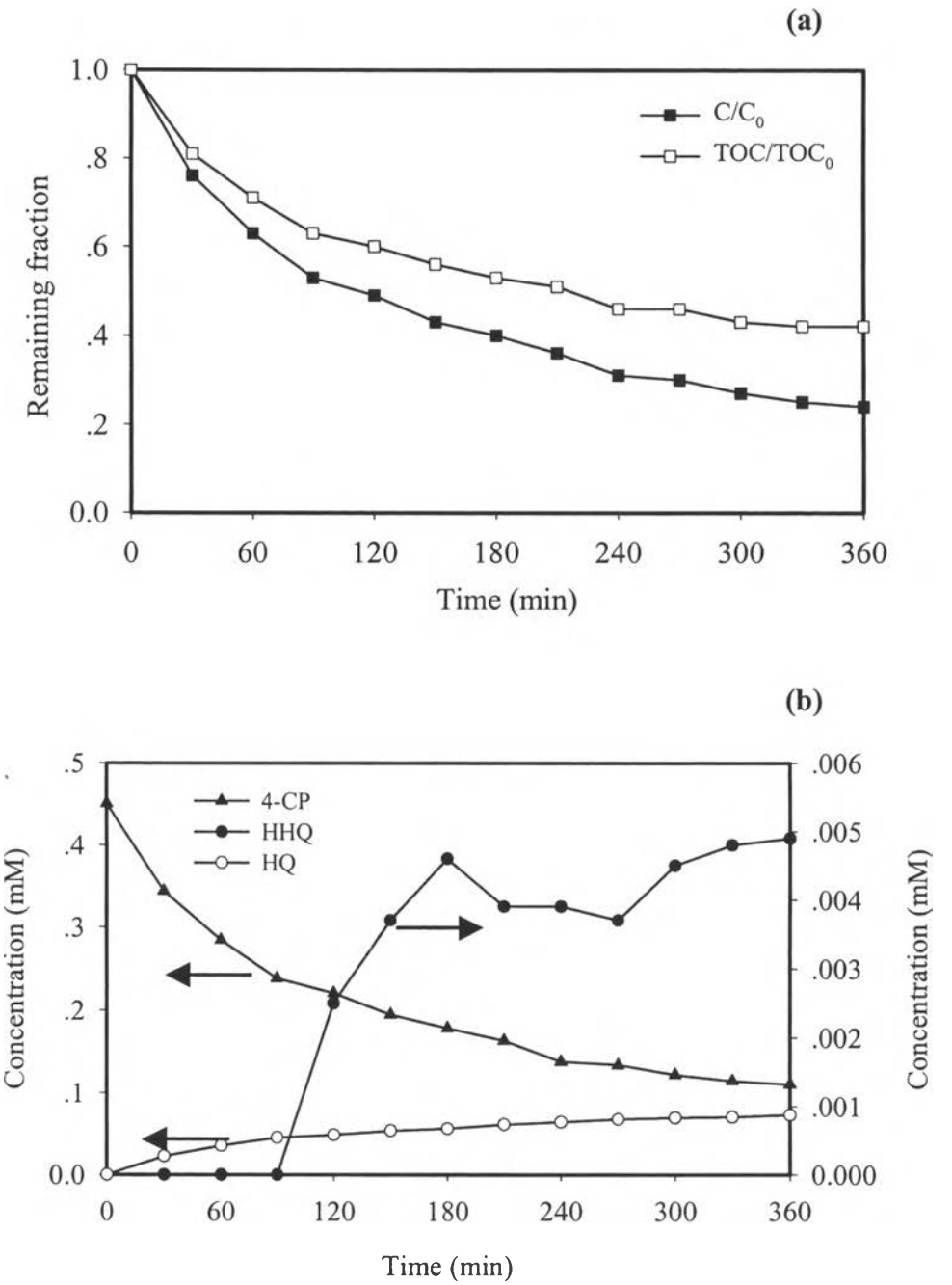

Figure 4.10 Photocatalytic degradation of 4-CP as a function of irradiation time using TiO_2 (Degussa P25) under the absence of dissolved oxygen (a) remaining fractions of 4-CP and TOC (b) concentrations of the intermediate products. Experimental conditions: 5 g/l catalyst, 0.5 mM 4-CP, 298 K and 5.5 initial pH.

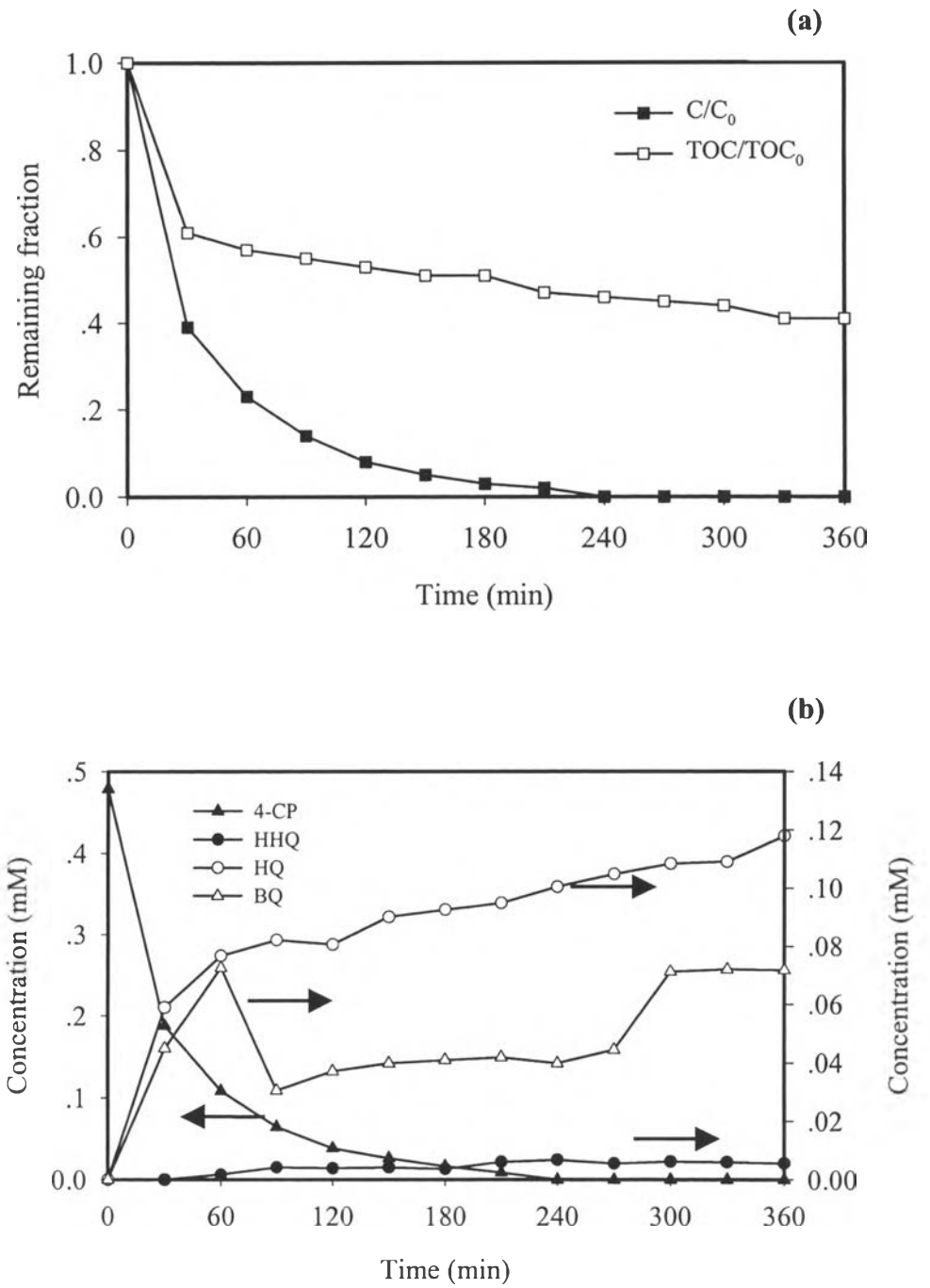

Figure 4.11 Photocatalytic degradation of 4-CP as a function of irradiation time using TiO_2 (sol-gel-1) under the absence of dissolved oxygen (a) remaining fractions of 4-CP and TOC (b) concentrations of the intermediate products. Experimental conditions: 5 g/l catalyst, 0.5 mM 4-CP, 298 K and 5.5 initial pH.

Table 4.3 Remaining fractions of TOC at the 360 minutes irradiation time.

Catalyst	TOC/TOC_0	
	Without dissolved oxygen	With dissolved oxygen
Without catalyst	0.76	0.62
TiO_2 (Degussa P25)	0.42	0.07
TiO_2 (sol-gel-1)	0.41	0.10
$1\%Pt/TiO_2$	0.27	0.20

4.2.1.4 Effect on solution pH

It was found experimentally from the previous work that the initial pH of 4-CP solution did not have a significant effect on both TOC removal rate and 4-CP degradation rate (Tharathonpisutthikul, 2000). The initial pH of 4-CP solution used in this study was 5.5. Because of the formation of HCl, the solution pH was lower to 4.5 after the irradiation time of 360 minutes. It is interesting to determine the effect of the solution pH on the 4-CP degradation rate again.

4.2.2 Photocatalytic Degradation of 4-CP with Pt/TiO_2

In this study, the photocatalytic degradation of 4-CP using 1% Pt/TiO_2 prepared by the first sol-gel method under either the presence or absence of dissolved oxygen was investigated. Figures 4.12 and 4.13 show the 4-CP degradation using Pt/TiO_2 with and without dissolved oxygen, respectively. Under the absence of dissolved oxygen, the three intermediate products, HQ, BQ and HHQ were generated but BQ was not observed for the system having dissolved oxygen. The presence of dissolved oxygen could enhance the degradation rates of 4-CP, TOC and the intermediate products as compared to the system having zero dissolved oxygen. As explained before, dissolved oxygen is responsible for the the formation of hydroxyl radicals which is very active to convert 4-CP to HQ, HHQ are finally CO_2.

Figure 4.14 shows the comparative photocatalytic activities of 4-CP degradation with different catalysts under the presence or absence of dissolved

oxygen. Compared to pure TiO_2, an addition of 1.0% Pt into TiO_2 could increase the photocatalytic activity when the system was operated under the absence of dissolved oxygen. Surprisingly, a significant decrease in the photocatalytic degradation of 4-CP was found that when 1% Pt was added in TiO_2 under the presence of dissolved oxygen. The results can be explained by the previous work reported by Blazkova *et al.* (1998) that an increase oxygen flow significantly enhanced the photocatalytic activity of phenol with Pt/TiO_2 but the oxygen flow larger than 5 dm^3/min under the given experimental conditions damaged the activity.

4.2.3 Photocatalytic Degradation of 4-CP with Ag/TiO_2

Effects of adding Ag to TiO_2 prepared by the first sol-gel method on the degradation of 4-CP were investigated systematically. A series of Ag/TiO_2 was prepared at different Ag loadings from 0.2-1.5 mol%. 0.5 mM 4-CP and 0.5 g/l catalyst were used. The degradation rates of 4-CP at different Ag loadings are shown in Figures 4.15-4.18. Compared to pure TiO_2 (sol-gel-1), an addition of Ag in TiO_2 does not alter the breakdown pathway of 4-CP. HQ was first formed and then degraded to form HHQ.

The remaining fractions of 4-CP and TOC are compared in Figure 4.19 and the values of remaining fractions of TOC at 360 minutes and the loadings are plotted to compare the effect of the Ag loadings on the TOC reduction rates as shown in Figure 4.20. It was clearly seen that the amount of Ag does not

significantly affect the degradation of 4-CP but has the effect on the intermediate products and TOC degradation. It was found that the 0.5 % Ag/TiO_2 has a minimum value of TOC at 360 minutes. With Ag greater than 0.5 mol %, the remaining TOC increases with increasing Ag loading. The less TOC indicates that more organic compounds react and convert into CO_2. The results indicate that a small amount of Ag added could improve the photocatalytic activity of TiO_2 and the optimum amount of Ag loading is 0.5 mol %. As can be seen from Figure 4.21, 0.5 % Ag/TiO_2 gives the highest photocatalytic activity in terms of the lowest of the remaining fraction of TOC at 360 minutes. It can be explained that a small amount of Ag on TiO_2 attributes to the acceleration of superoxide radical anion, $O_2^{\bullet-}$, formation resulting in decreasing the recombination process as well as enhancing the

oxidation reaction by its oxidative property. But when the amount of Ag increases to a certain level, the photoelectron will transfer from the semiconductor to metal particles as well as the decrease of $O_2^{\bullet-}$ resulting in the increase of recombination and lower the photocatalytic activity (Blazkova *et al.*, 1998). Another possible explanation is that Ag increases the rate of direct hole oxidation pathway leading to improving the photocatalytic activity (Ilisz and Dombi, 1999).

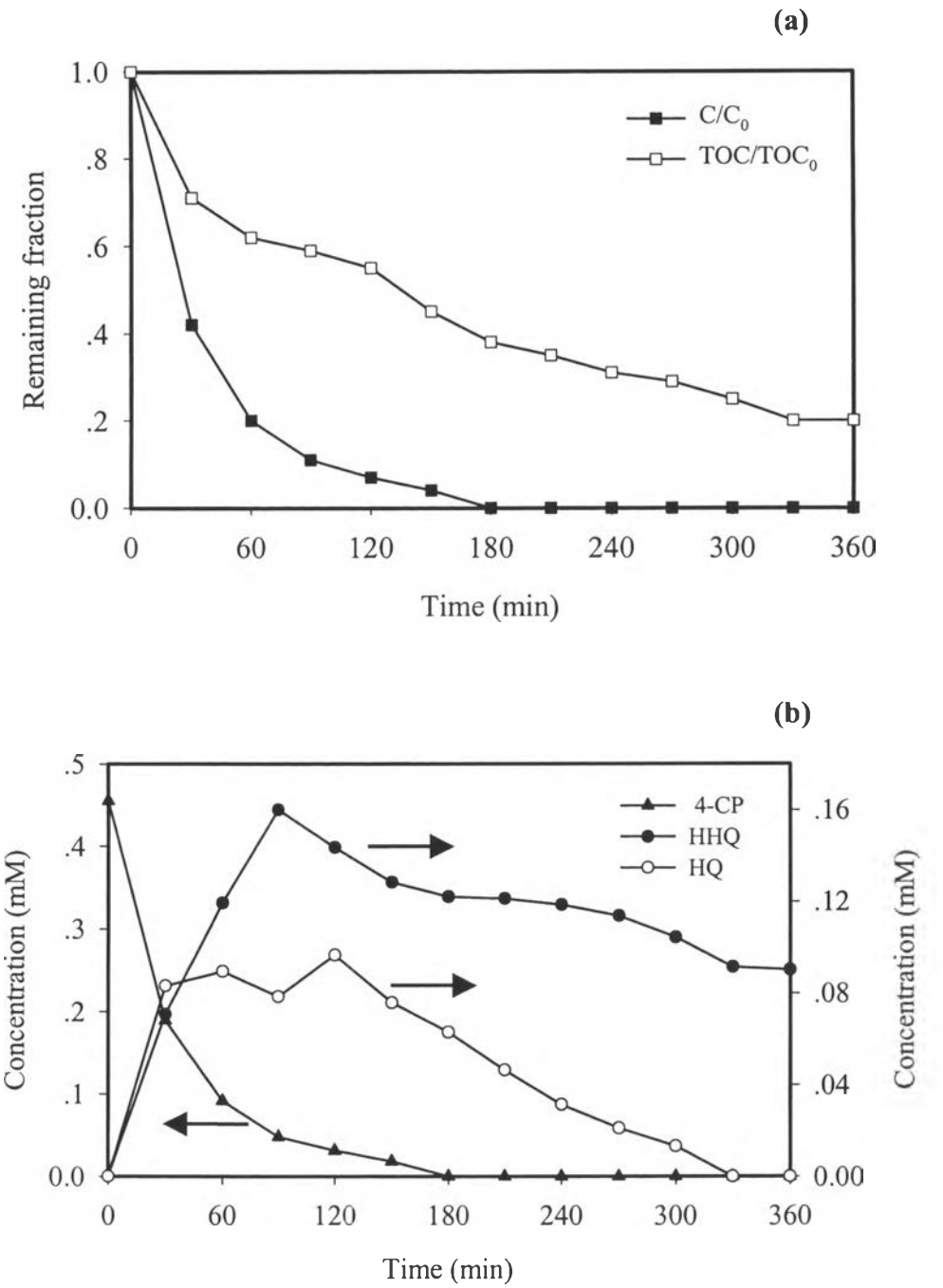

Figure 4.12 Photocatalytic degradation of 4-CP as a function of irradiation time using 1.0% Pt/TiO_2 under the presence of dissolved oxygen (a) remaining fractions of 4-CP and TOC (b) concentrations of the intermediate products. Experimental conditions: 5 g/l catalyst, 0.5 mM 4-CP, 298 K and 5.5 initial pH.

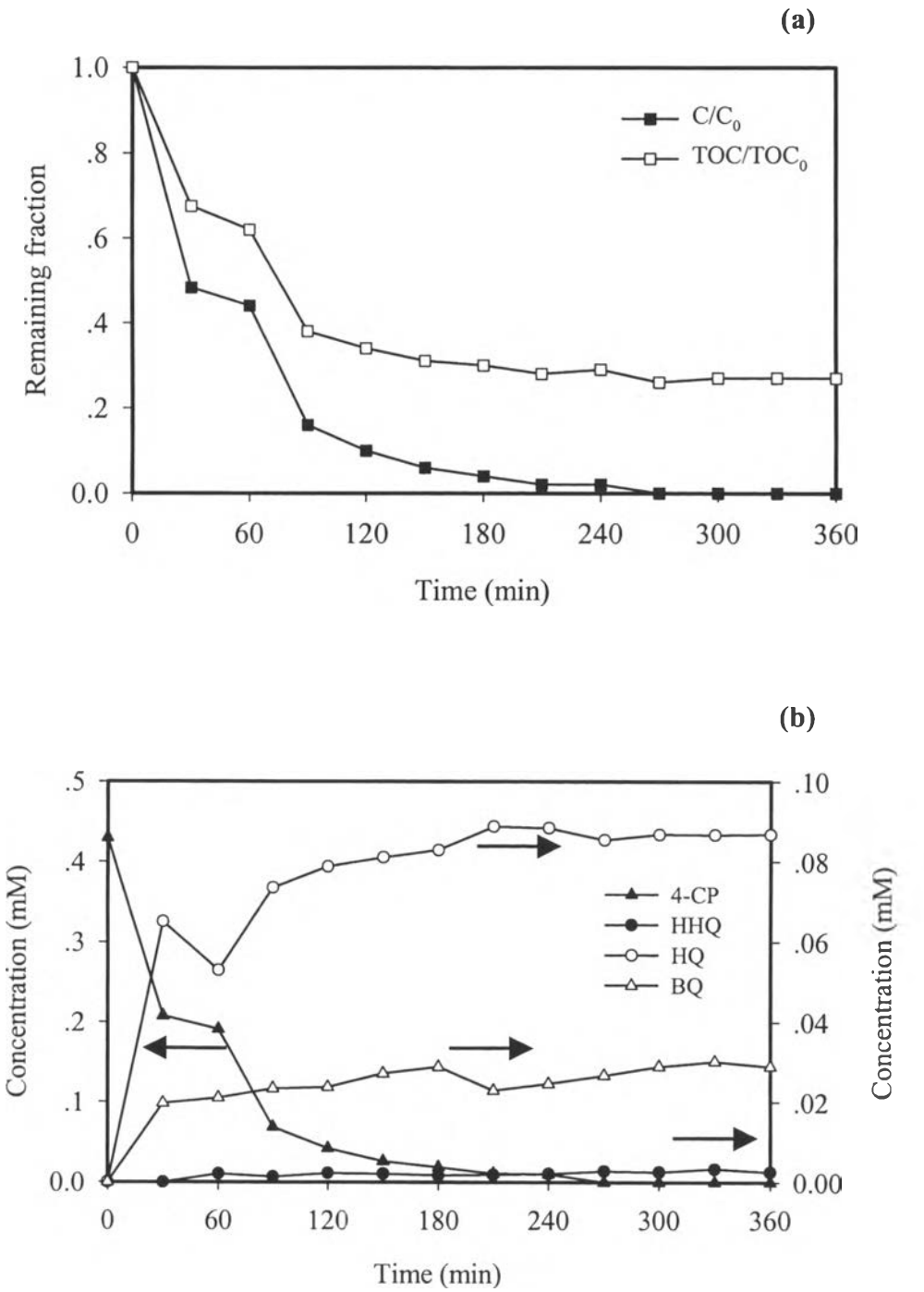

Figure 4.13 Photocatalytic degradation of 4-CP as a function of irradiation time using 1.0% Pt/TiO_2 under the absence of dissolved oxygen (a) remaining fractions of 4-CP and TOC (b) concentrations of the intermediate products. Experimental conditions: 5 g/l catalyst, 0.5 mM 4-CP, 298 K and 5.5 initial pH.

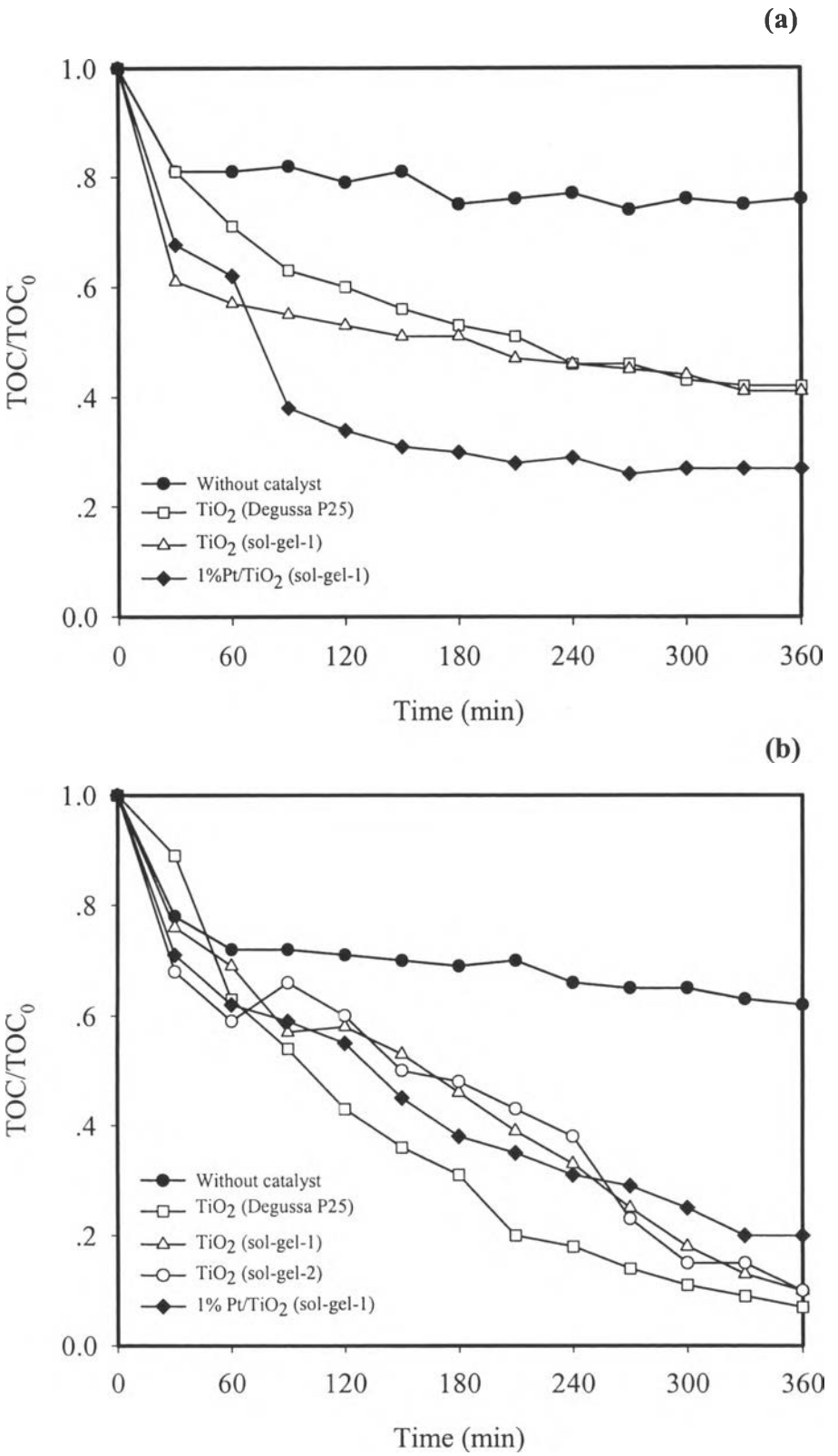

Figure 4.14 Comparing the remaining fraction of TOC as a function of time for different catalysts (a) under the presence of dissolved oxygen (b) under the absence of dissolved oxygen.

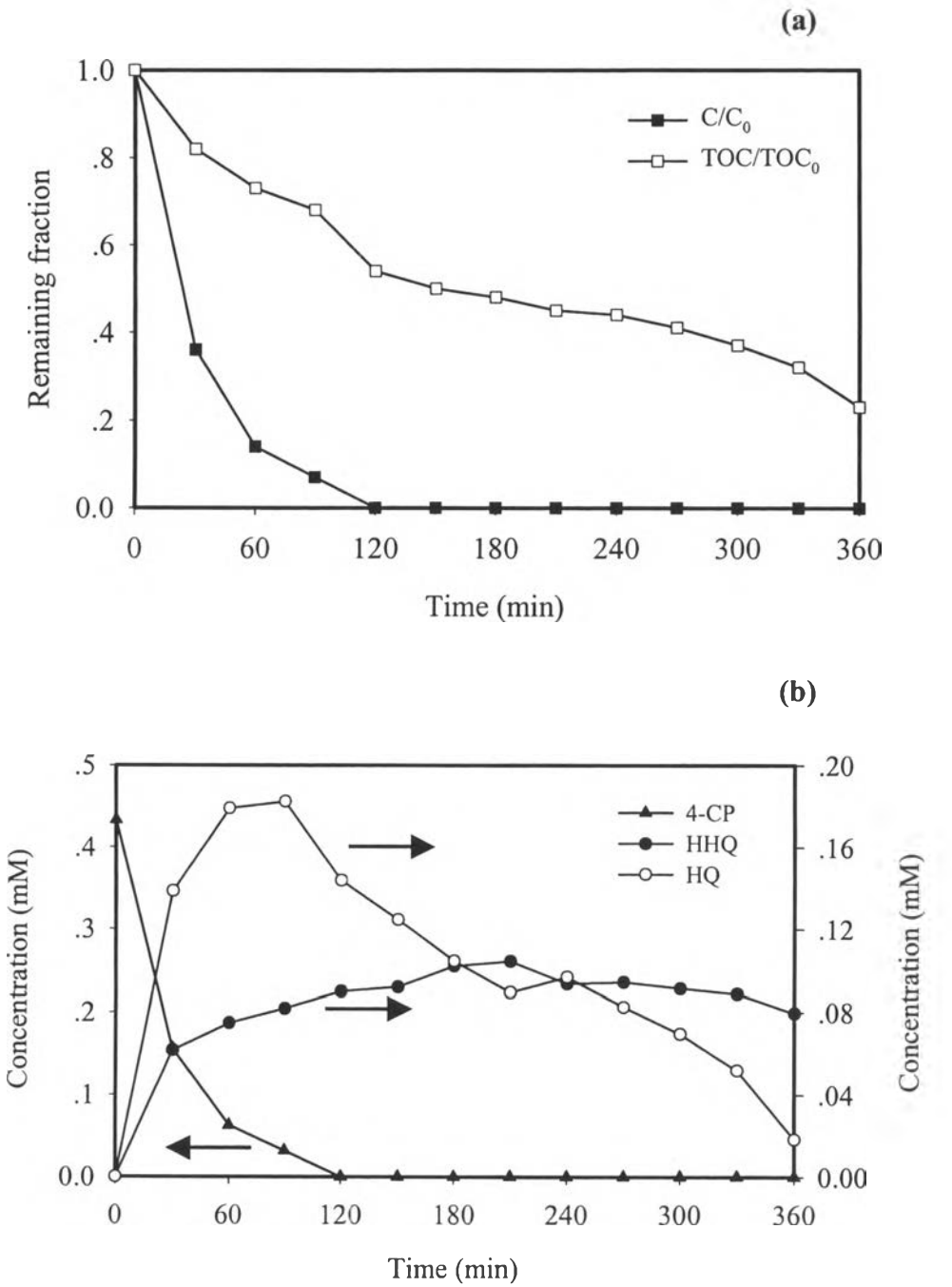

Figure 4.15 Photocatalytic degradation of 4-CP as a function of irradiation time using 0.2% Ag/TiO_2 under the presence of dissolved oxygen (a) remaining fractions of 4-CP and TOC (b) concentrations of the intermediate products. Experimental conditions: 5 g/l catalyst, 0.5 mM 4-CP, 298 K and 5.5 initial pH.

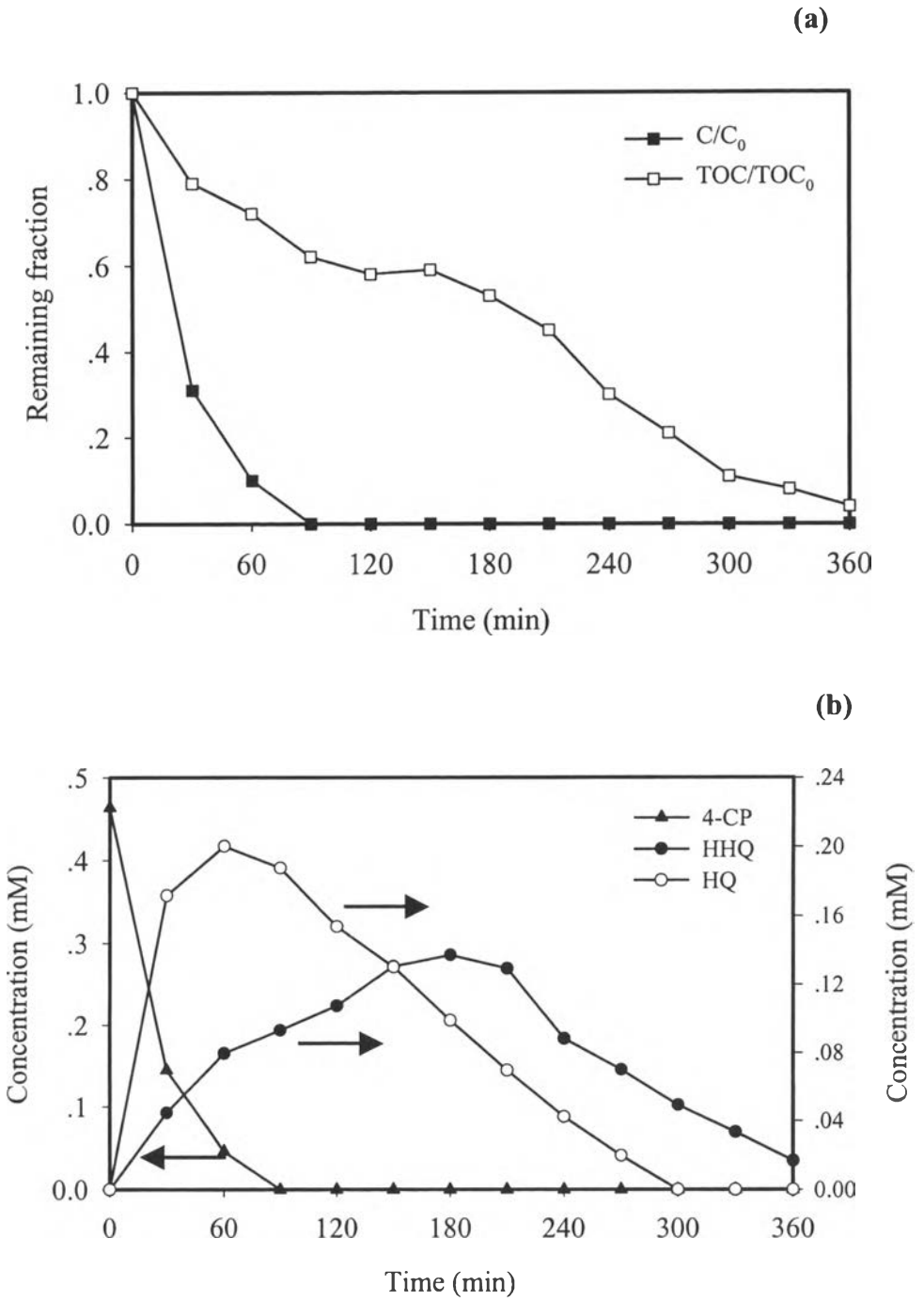

Figure 4.16 Photocatalytic degradation of 4-CP as a function of irradiation time using 0.5% Ag/TiO_2 under the presence of dissolved oxygen (a) remaining fractions of 4-CP and TOC (b) concentrations of the intermediate products. Experimental conditions: 5 g/l catalyst, 0.5 mM 4-CP, 298 K and 5.5 initial pH.

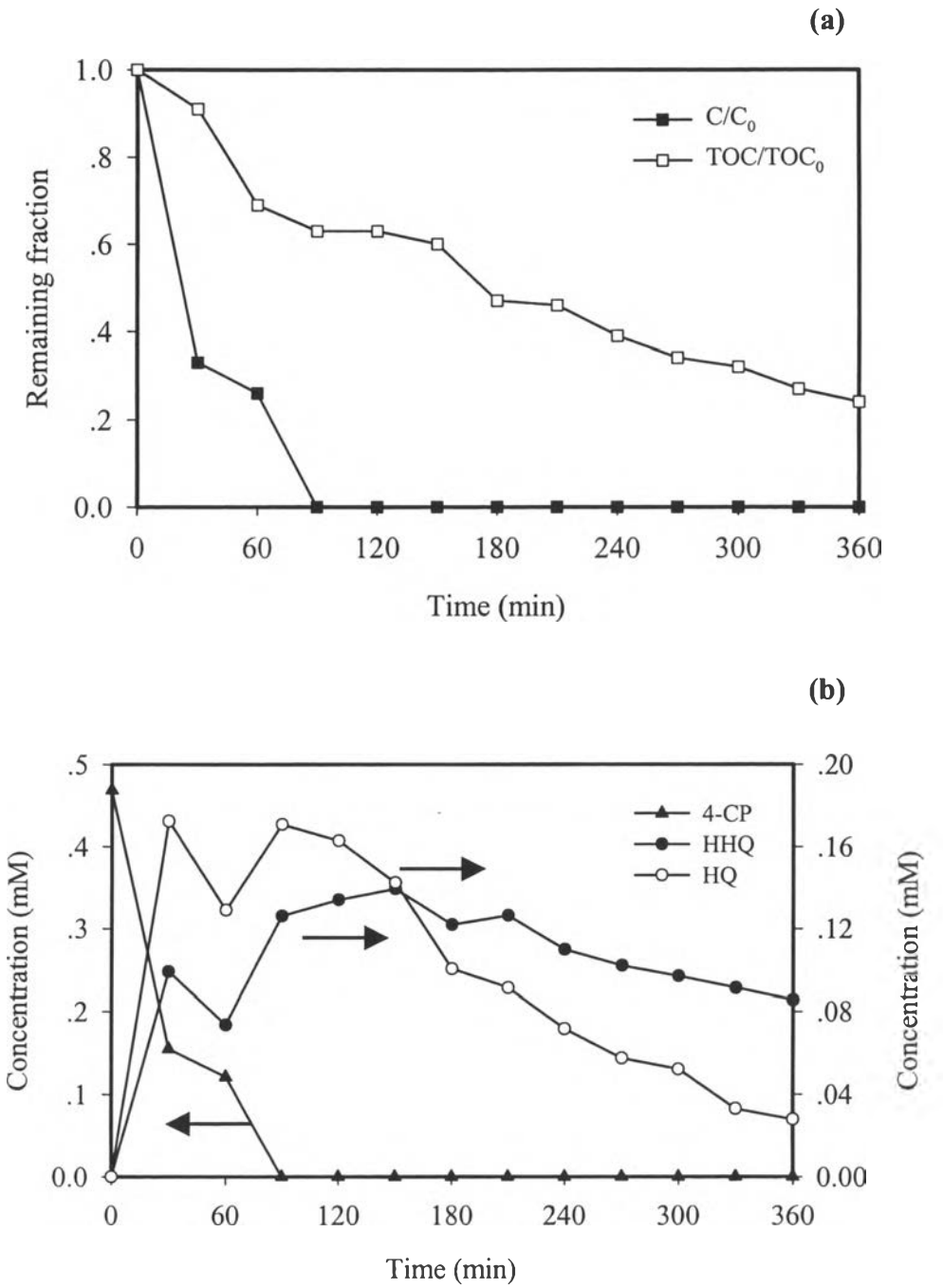

Figure 4.17 Photocatalytic degradation of 4-CP as a function of irradiation time using 1.0% Ag/TiO_2 under the presence of dissolved oxygen (a) remaining fractions of 4-CP and TOC (b) concentrations of the intermediate products. Experimental conditions: 5 g/l catalyst, 0.5 mM 4-CP, 298 K and 5.5 initial pH.

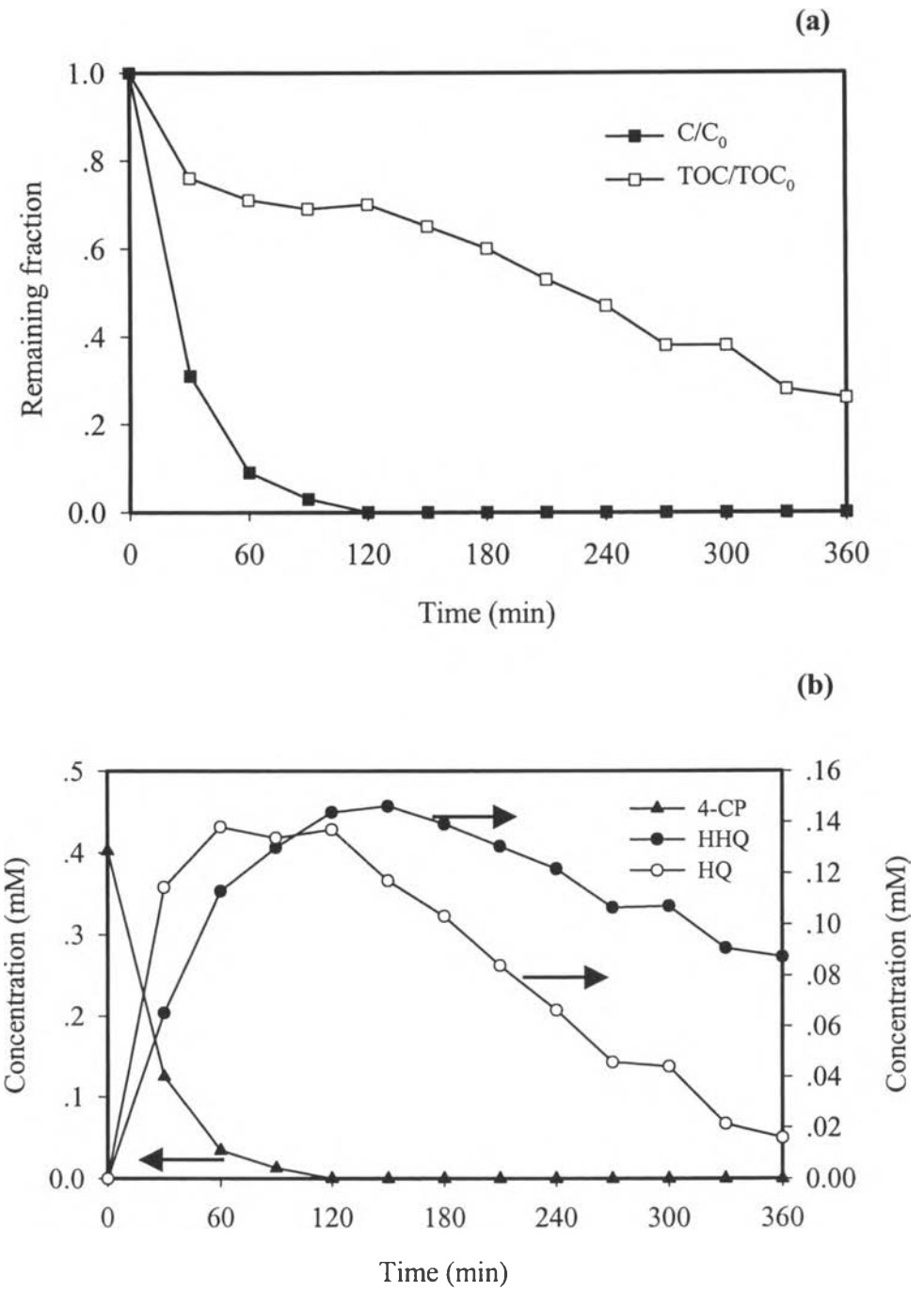

Figure 4.18 Photocatalytic degradation of 4-CP as a function of irradiation time using 1.5% Ag/TiO_2 under the presence of dissolved oxygen (a) remaining fractions of 4-CP and TOC (b) concentrations of the intermediate products. Experimental conditions: 5 g/l catalyst, 0.5 mM 4-CP, 298 K and 5.5 initial pH.

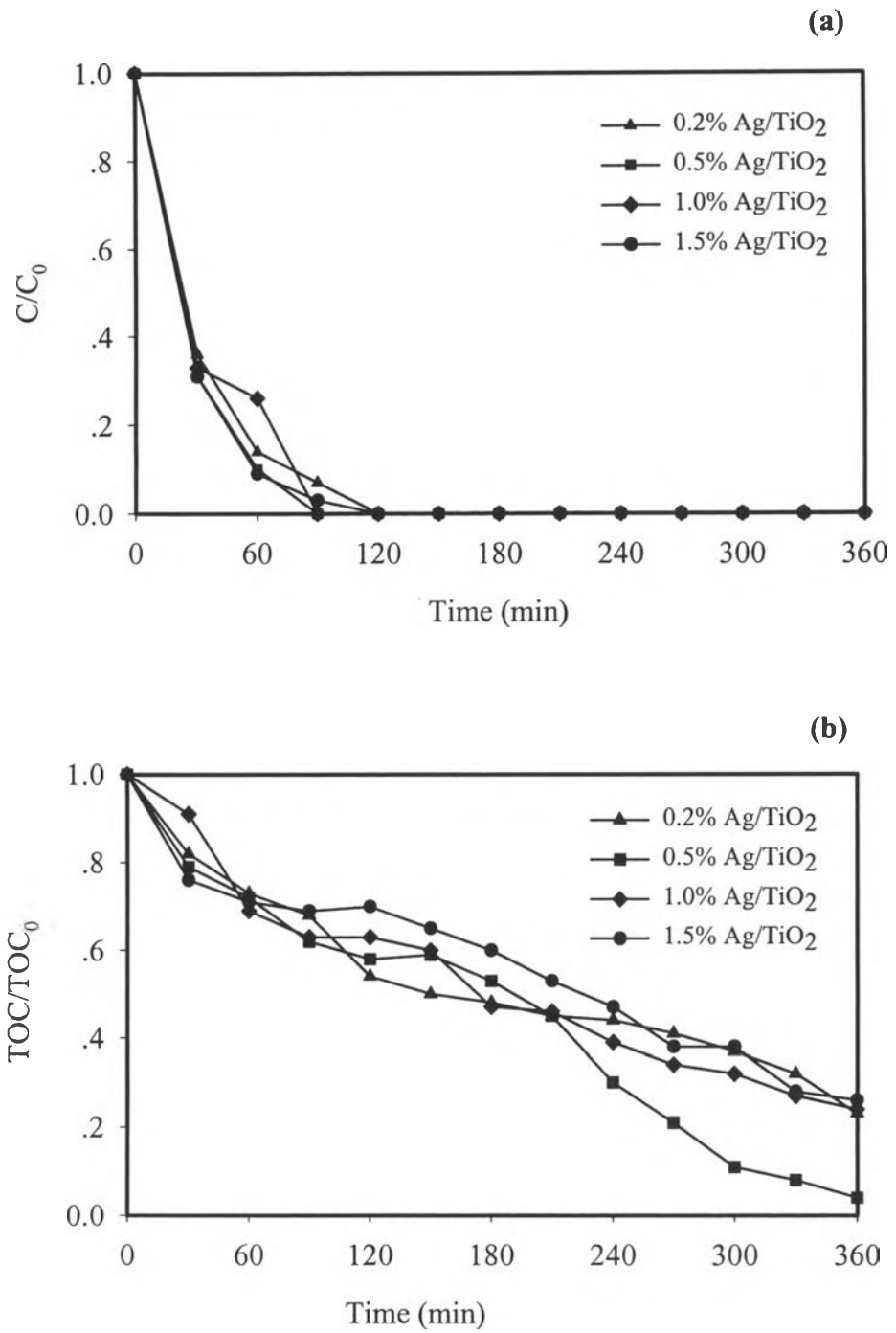

Figure 4.19 Camparison of remaining fraction of (a) 4-CP and (b) TOC for different %Ag loadings.

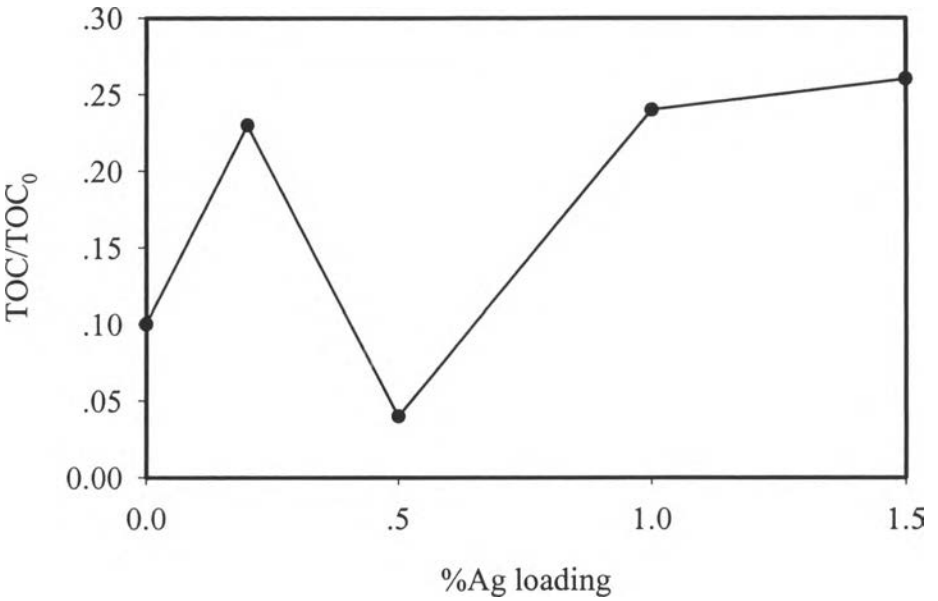

Figure 4.20 Remaining fraction of TOC at 360 minnutes for different %Ag loadings in TiO_2 under the presence of dissolved oxygen.

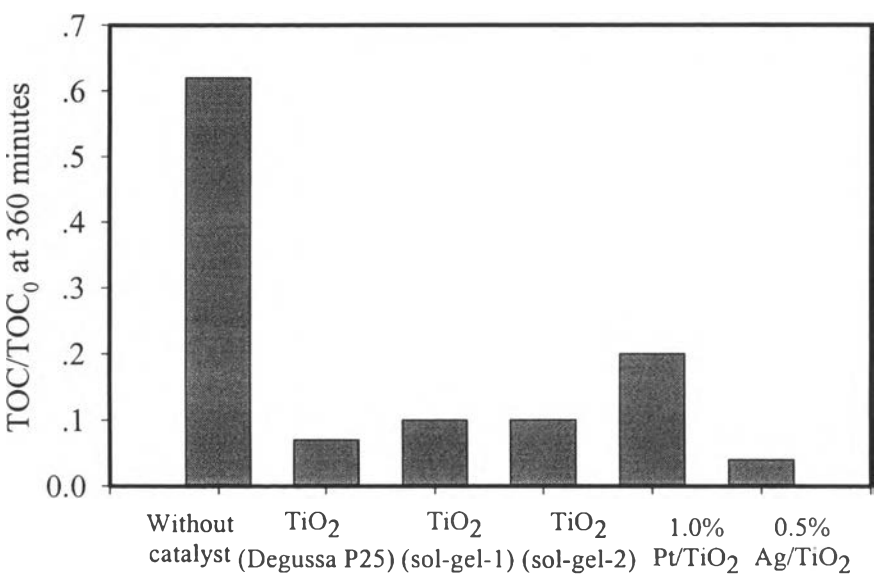

Figure 4.21 Remaining fraction of TOC at 360 minutes for different catalysts and under the presence of dissolved oxygen.

4.2.4 Photocatalytic Degradation Pathway of 4-CP

During the photocatalytic degradation with each catalyst, the aromatic intermediates were detected by HPLC. All species in the solution were identified by comparing the retention times of the observed peaks with the retention times of the standard peaks of know chemicals. The structural formulas of identified compounds are shown in Figure 4.22. For the studied catalysts, the two intermediate products generated during the 4-CP degradation are hydroquinone (HQ) and hydroxyhydroquinone (HHQ) when the photocatalytic system was operated under the presence of dissolved oxygen. However, TiO_2 (sol-gel-1) and Pt/TiO_2 with aerated nitrogen condition or without dissolved oxygen generated three intermediate products are HQ, HHQ, and benzoquinone (BQ).

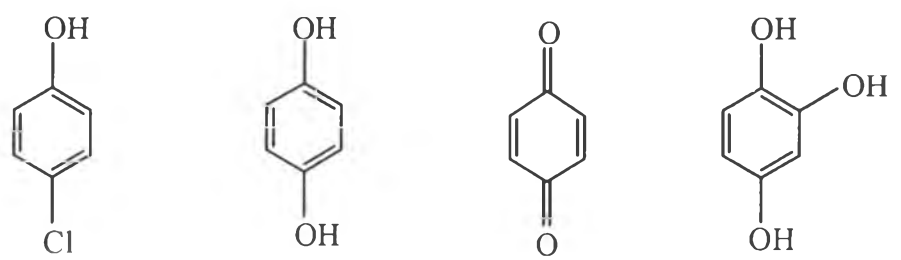

4-chlorophenol Hydroquinone Benzoquinone Hydroxyhydroquinone

Figure 4.22 Molecular structures of species present during the photocatalytic degradation of 4-CP.

Figure 4.6 (a) illustrates the 4-CP degradation using TiO_2 (Degussa P25) with dissolved oxygen. The figure indicates that the concentration of HHQ increases almost linearly until the irradiation time of 150 minuts whereas the concentration of HQ increases and reaches a maximum after 90 minutes before its concentration decreases progressively. The shape of the HQ curve is typical for a compound formed as a primary intermediate in a consecutive reaction:

$$A \rightarrow B \rightarrow C \rightarrow D \qquad (4.1)$$

For a better understanding of the degradation pathway of 4-CP under the presence of the dissolved oxygen condition, an analogous experiment was carried out for the degradation of HQ under the same experimental conditions as used for the irradiation of 4-CP. Figure 4.23 illustrates a decrease in the concentration of HQ as a function of the irradiation time observed during the photocatalytic degradation of 0.5 mmol/l HQ. HHQ is the only detected intermediate product during the photocatalytic degradation of HQ. Accordingly, the proposed reaction pathway for the photocatalytic degradation of 4-CP is shown in Figure 4.24. 4-CP is oxidized firstly into HQ and HQ is further oxidized into HHQ. Eventually, HHQ is mineralized to CO_2 and water.

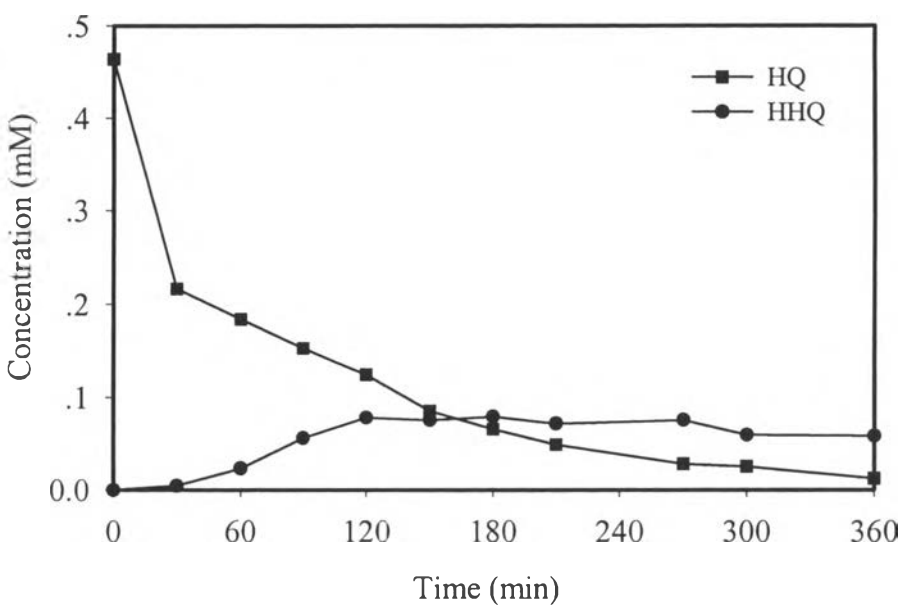

Figure 4.23 Photocatalytic degradation of HQ as a function of irradiation time using TiO_2 (Degussa P25) with oxygen aeration. Experimental conditions: 0.5 g/l catalyst, 0.5 mM HQ and 298 K.

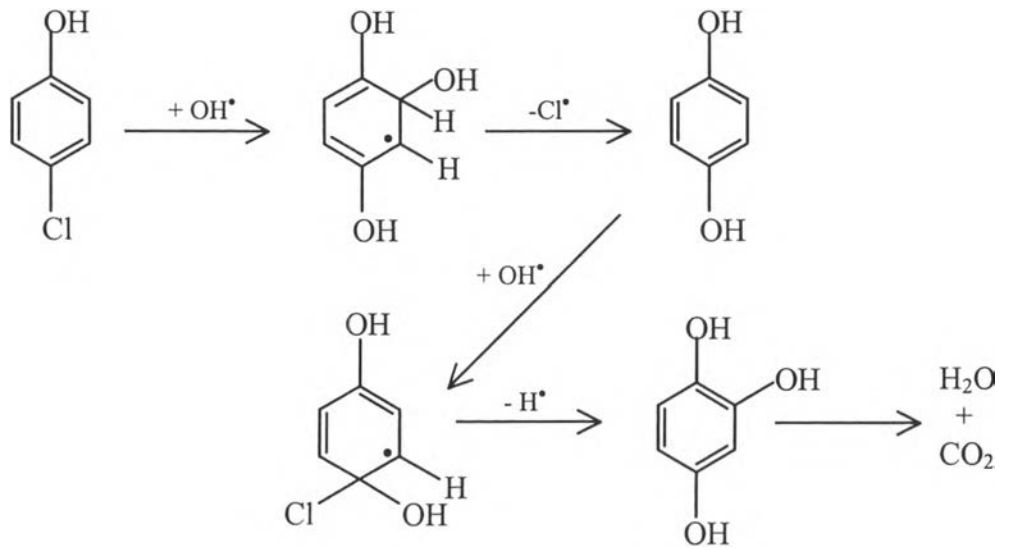

Figure 4.24 Reaction pathway for the photocatalytic degradation of 4-CP under the presence of dissolved oxygen.

Under the presence of dissolved oxygen, hydroxyl radical can be formed by the following equations:

$$H_2O + h^+ \rightarrow OH^\bullet + H^+ \quad (4.2)$$

$$O_2 + e^- \rightarrow O_2^{\bullet-} \quad (4.3)$$

$$2H_2O + O_2^{\bullet-} \rightarrow 2H_2O_2 \quad (4.4)$$

$$H_2O_2 \rightarrow 2OH^\bullet \quad (4.5)$$

For the free-dissolved oxygen system, there is small amount of hydroxyl radical formed since it is only generated from equation (4.2). Consequently, the oxidization rate of HQ to HHQ decreases. Under the presence of mind oxidizing agent, oxidization of HQ produces BQ and the reaction is reversible (Morrison and Boyd, 1992). As seen from Figure 4.13, there is small amount of HHQ while the concentration of HQ and BQ are relatively constant. Accordingly, the proposed reaction pathway for the photocatalytic degradation of 4-CP under the absence of oxygen is shown in Figure 4.25.

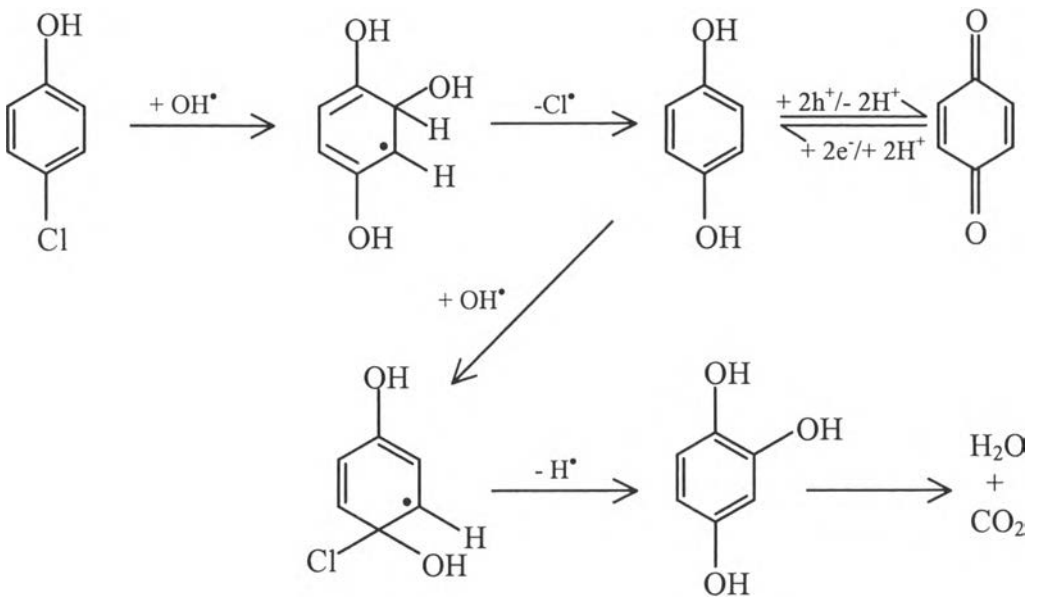

Figure 4.25 Reaction pathway for the photocatalytic degradation of 4-CP under the absence of dissolved oxygen.